

NUMERICAL INVESTIGATION OF THE CHARACTERISTICS OF AN INHOMOGENEOUS FLUIDIZED BED

A. M. Bubenchikov and A. V. Starchenko

UDC 621.391:66.096.5

A mathematical model for a numerical investigation of the processes of mixing of dispersed material in fluidized beds is presented. Results of comparing the calculations with experimental data on the expansion and porosity of a thin inhomogeneous fluidized bed are given.

The technology of liquefying dispersed materials has widespread application in the chemical industry and metallurgy. In recent years, work on investigating fluidized beds (FB) in power engineering, used for burning of coals in boiler unit furnaces, has been carried out. The effect from using FB in processes with chemical transformations is primarily attained due to active mixing of phases and components comprising the suspended layer. The intensity of the processes of mixing is substantially determined by the liquefaction regime. Depending on the dimensions and properties of the particles and the rate of the carrier medium feed, different regimes of the liquefaction of the solid phase can be realized: nucleate, piston, turbulent, etc., and their intermediate forms [1].

Experimental investigations of fluidized beds consist in developing small-scale devices and analyzing the laws of distribution of the solid phase throughout the apparatus volume (determination of the expansion ratio for the bed and the average porosity along its height) as well as in the efficiency of operation of heat transfer surfaces immersed in the FB. In this case a serious problem connected with ensuring physical similarity of the natural and laboratory processes arises. Nevertheless, information on the hydrodynamic structure of the FB in the model apparatus turns out to be extremely useful in carrying out research work on designing real objects. The results of physical modeling are especially important for the development of numerical models, which basically enable one to analyze the processes of mixing in devices of all configurations and scales. Increasingly powerful computers and the current state-of-the-art in mechanics of disperse systems make these calculations possible.

The difficulties of a theoretical study of FB are associated with the pulsation nature of the motion of the particles and the liquefying agent in the bed. For example, the turbulent regime of the liquefaction of a dispersed material is superficially similar to the turbulent regime of the motion of a continuous medium. Nevertheless, the nature of hydrodynamic pulsations in both cases is completely different. Whereas some experience in investigating the structure of pulsation fields has been accumulated in turbulence theory, it is clearly lacking in disperse system mechanics as applied to the phenomenon of a fluidized bed. This complicates the problem of mathematical modeling of FB. When carrying out numerical modeling of hydrodynamically unstable processes, it is quite helpful to use, together with experimental information and phenomenological notions, a set of base equations expressing the basic laws of conservation. In turbulent flow mechanics the role of a theoretical base is played by an expanded system of Navier-Stokes equations, which in principle enables us to obtain all the characteristics of turbulence. Moreover, there are examples of direct modeling of turbulence based on such a system of equations. However, using this approach has substantial limitations associated with the need to resolve small-scale structures and high-frequency hydrodynamic pulsations. The spectrum of frequencies and scales arising in the fluidized bed provides substantially greater possibilities for carrying out direct numerical modeling of FB.

The present work proposes a general approach enabling us to determine the basic characteristics of a fluidized bed no irrespective of the fluidization regime. The approach consists in using the equations of heterogeneous media mechanics [2] and carrying out direct numerical modeling of two-dimensional nonstationary motion of a gas and a

Scientific-Research Institute of Applied Mathematics and Mechanics, Tomsk. Translated from *Inzhenerno-Fizicheskii Zhurnal*, Vol. 65, No. 2, pp. 178-184, August, 1993. Original article submitted March 25, 1992.

dispersed material in a fluidized bed. The numerical model was checked on experimental data obtained in analyzing thin nonhomogeneous isothermal liquefied beds [3].

We consider the nonstationary flow of a gas-solid particle mixture in a flat vertical channel (see, for example, Fig. 2; the x axis is directed vertically, and the y axis transversely to the channel). Here, it is assumed that the particles are spherical and of the same size and the particle material density substantially exceeds the carrier medium density. The interphase dynamic interaction is described by the resistance force. Moreover, for the dispersed phase we consider forces acting in a local group of particles due to their compaction. Since the volume fraction of particles in the flow is large we will take into account shear stresses in the particle continuum according to [4].

By using these assumptions the basic system of equations in the theory of interacting and interpenetrating continua [2] can be written in the following manner:

$$\frac{\partial \rho_i}{\partial t} + \frac{\partial}{\partial x} (\rho_i U_i) + \frac{\partial}{\partial y} (\rho_i V_i) = 0, \quad (1)$$

$$\begin{aligned} & \frac{\partial}{\partial t} (\rho_i U_i) + \frac{\partial}{\partial x} (\rho_i U_i U_i) + \frac{\partial}{\partial y} (\rho_i V_i U_i) = -\delta_{1i} \frac{\partial p}{\partial x} + \\ & + 2 \frac{\partial}{\partial x} \left(\mu_i \alpha_i \frac{\partial U_i}{\partial x} \right) + \frac{\partial}{\partial y} \left(\mu_i \alpha_i \frac{\partial U_i}{\partial y} \right) + \frac{\partial}{\partial y} \left(\mu_i \alpha_i \frac{\partial V_i}{\partial x} \right) - \end{aligned} \quad (2)$$

$$- \frac{2}{3} \frac{\partial}{\partial x} \left[\mu_i \alpha_i \left(\frac{\partial U_i}{\partial x} + \frac{\partial V_i}{\partial y} \right) \right] + F_{xi} - \rho_i g - \delta_{2i} G \frac{\partial \alpha_i}{\partial x},$$

$$\begin{aligned} & \frac{\partial}{\partial t} (\rho_i V_i) + \frac{\partial}{\partial x} (\rho_i U_i V_i) + \frac{\partial}{\partial y} (\rho_i V_i V_i) = -\delta_{1i} \frac{\partial p}{\partial y} + \\ & + \frac{\partial}{\partial x} \left(\mu_i \alpha_i \frac{\partial V_i}{\partial x} \right) + 2 \frac{\partial}{\partial y} \left(\mu_i \alpha_i \frac{\partial V_i}{\partial y} \right) + \frac{\partial}{\partial x} \left(\mu_i \alpha_i \frac{\partial U_i}{\partial y} \right) - \end{aligned} \quad (3)$$

$$\begin{aligned} & - \frac{2}{3} \frac{\partial}{\partial y} \left[\mu_i \alpha_i \left(\frac{\partial U_i}{\partial x} + \frac{\partial V_i}{\partial y} \right) \right] + F_{yi} - \delta_{2i} G \frac{\partial \alpha_i}{\partial y}, \\ & p = \rho_1^0 RT. \end{aligned} \quad (4)$$

Here $i = 1$ is the gas, $i = 2$ is the dispersed phase; $\rho_i = \rho_1^0 \alpha_i$, α_i is the volume fraction of the i -th phase, $\alpha_1 + \alpha_2 = 1$; μ_i is the viscosity factor; U_i , V_i are the corresponding velocity vector components of the i -th phase; p is the pressure; ρ_1^0 is the density of the gas ($i = 1$) or of the particle material ($i = 2$); R , T are the gas constant and the temperature.

The last terms in the right-hand sides of Eqs. (2) and (3) are the interphase pressure in the particle medium and contribute to equalization of the solid phase concentrations in zones of significant gradients of these quantities. In the present work the following relation [4] is used for the modulus of stresses of the dispersed phase G :

$$G = \exp[-c(\varepsilon - \varepsilon^*)], \quad (5)$$

where $c = 600$, $\varepsilon^* = 0.376$, and $\varepsilon = \alpha_1$ is the porosity for the conditions considered in the present work.

We note that other models determining the dispersed phase pressure also exist, for example, [2]. However, relation (5) is proposed in [4] for describing the state of a two-phase medium precisely in a fluidized bed.

The dynamic interaction between the phases is determined by the following relations:

$$F_{x1} = -F_{x2} = \beta(U_2 - U_1), \quad F_{y1} = -F_{y2} = \beta(V_2 - V_1). \quad (6)$$

The coefficient of interphase friction β is determined for $\alpha_1 \leq 0.8$ using the Ergun equation [1]

$$\beta = 150 \frac{\mu_1 \alpha_2^2}{(\alpha_1 d_p)^2} + 1.75 \frac{\rho_1^0 |W_1 - W_2| \alpha_2}{\alpha_1 d_p}, \quad (7)$$

and for $\alpha_1 \geq 0.8$ using the following law:

$$\beta = \frac{3}{4} c_D \frac{|W_1 - W_2| \rho_1^0 \alpha_2}{d_p} \alpha_1^{-2.65}, \quad (8)$$

where

$$c_D = \frac{24}{Re} (1 + 0.15 Re^{0.687}), \quad Re \leq 1000;$$

$$c_D = 0.44, \quad Re > 1000; \quad Re = \frac{|W_1 - W_2| d_p \rho_1^0 \alpha_1}{\mu_1},$$

d_p is the particle diameter.

The viscosity of the dispersed phase μ_2 is of substantial importance in studying nonstationary motions of gas-particle mixtures for high values of the volume fraction of particles ($\alpha_2 \geq 0.1$). For example, in [4] with the viscosity $\mu_2 = 0.5$ Pa·sec good agreement of calculations with the experimental data on the frequency of emergence of "bubbles" in a flat isothermal fluidized bed is obtained using a model analogous to the one described above. This value of viscosity was determined by the authors of [4] experimentally. In the present work the value of μ_2 is chosen using the recommendations of [1], according to which $\mu_2 = 1.3$ Pa·sec for the conditions considered by us.

A uniform gas velocity profile and the no-flow condition for particles were used as boundary conditions on the inlet boundary (a distribution grid or a porous plate). On the outlet boundary (the superbed space) moderate boundary conditions were used for all quantities, and on the lateral surfaces the no-flow conditions for the particles and the resistances of the heterogeneous medium flow according to [1] were used, and the adherence conditions were used for the carrier medium. It was assumed that at the initial instant the gas is at rest and the particles form a stationary granular bed of bulk density with the height H_0 .

The problem considered was solved numerically on nonuniform checkerboard grids. The initial differential equations were discretized using the control volume method [5]. The system of algebraic equations obtained using an implicit approximation of the nonstationary equations of motion and a hybrid scheme for the convective terms was solved by the Gauss-Seidel iteration method. To determine the pressure, a SIMPLE algorithm was used [5]. Convergence of the computational algorithm was monitored at each time step using the maximum discrepancy determined for each of the transport equations and the value of the carrier medium flow rate and the pressure correction. The given algorithm gives a numerical solution over the entire zone in question without distinguishing any peculiarities ("bubbles," clusters) arising as the air goes through a layer of the initially stationary material.

The results of calculations of a thin inhomogeneous fluidized bed and comparison with the experimental data [3] are given below. From the series of experiments carried out on filling of sand and magnesite particles of various sizes and stationary beds of various heights we chose results related to a 0.01-m stationary bed formed from sand particles with an average size of 326 μm . The rate u_f of the gas liquefying the particles was 0.314, 0.544, and 0.76 m/sec, which is substantially larger than the minimum fluidization rate. The calculations of the variants given below are performed on grids with the number of nodes 30×20 using a nonstationary two-dimensional model of the motion of a heterogeneous mixture. The integration step over the time coordinate was determined by the character of the spatial distribution of the solid phase and was of the order of $10^{-2} - 10^{-3}$ sec.

As the calculations showed, features characterizing different liquefaction regimes are observed as the air goes through the layer of the initially stationary material. At first a uniform expansion of the layer is observed, and then bubbles (high-porosity zones) form, which gradually filled the entire cross section because of their increasing sizes, so that high-porosity layers alternated with portions of particle accumulation. These structures disintegrated further and random mixing of dispersed material masses (the turbulent regime of liquefaction) arose. In all the variants, formation of clusters of various sizes (zones with a solid phase density close to dense filling) was noted, which moved to the upper boundary of the fluidized bed as whole structures. The largest of them created conditions favorable for the outburst of mixture masses adjoining from below because of their interaction with the walls or disintegration, due to which the particles were ejected into the superbed space. After the state of the disperse system reached the turbulent regime of fluidization, the mixing process was more stable. It was at this stage of the calculations

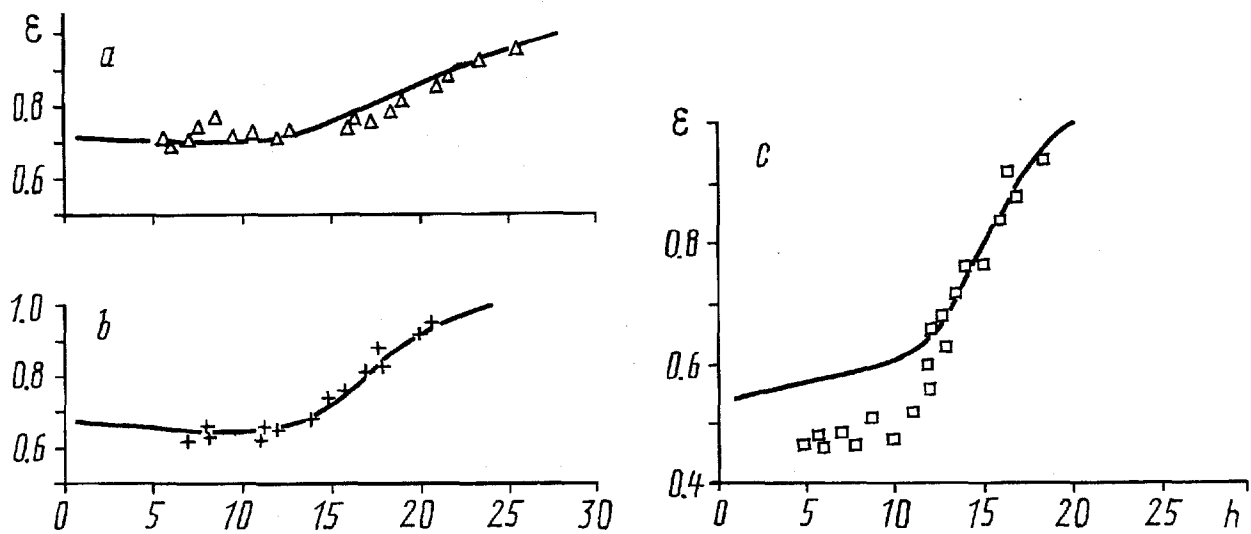


Fig. 1. Porosity distribution along the fluidized bed height. h , mm.

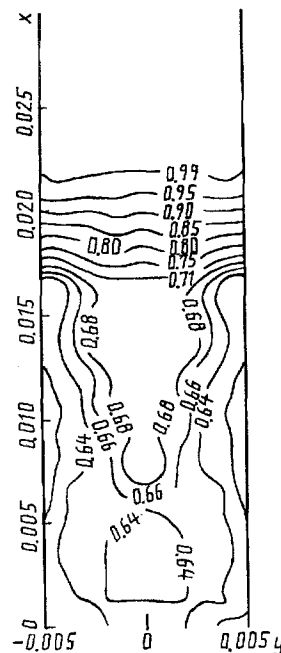


Fig. 2. Lines of constant porosity in the apparatus cross section, $u_f = 0.544$ m/sec. x, y , m.

that the characteristics of the bed were averaged over time. In parallel with this the values of porosity were also averaged over the bed width.

Figure 1 gives the results of the calculations of porosity, averaged over the channel width and time (solid curves) and the experimental data [3] (symbols). Here a, b, and c correspond to the cases $u_f = 0.76, 0.544,$ and 0.314 m/sec respectively. In all the variants the calculations give good prediction of the magnitude of the bed expansion. Furthermore, as the figure shows, in the first two cases (a, b) complete agreement between the calculated and experimental data is observed. The last variant (c) gives good agreement in the upper and middle part of the bed. However, in the lower zone the calculated values of porosity are larger than the measured ones. Increasing the calculation time did not lead to agreement between the results of the calculations and the experimental data. The differences can be explained by the inadequacy of modeling the forces acting in a dispersed phase whose density is close to dense filling (the last terms in Eqs. (2) and (3)) and also by possible differences in the conditions of the laboratory and numerical experiment. The latter is explained by the following fact. As was already mentioned above

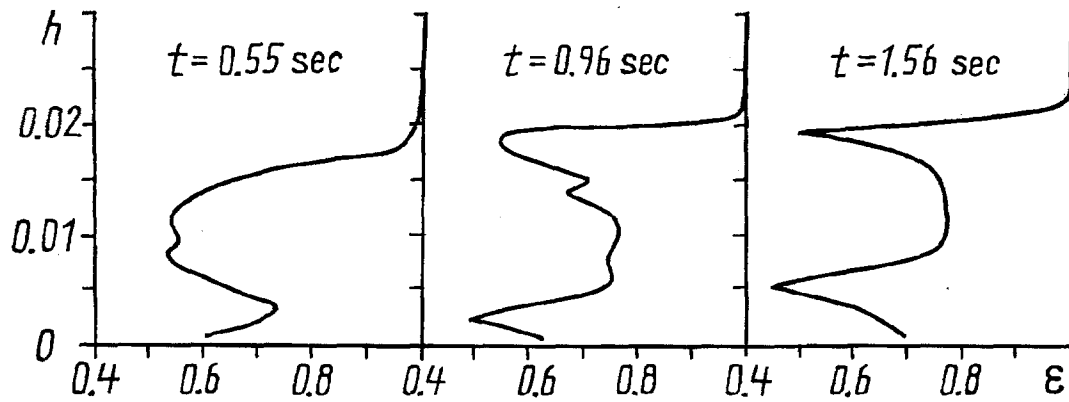


Fig. 3. Change in the porosity distribution over height with time, $u_f = 0.544$ m/sec. h , m.

the calculations were performed with the height $H_0 = 0.01$ m for the filling bed, which corresponds to a quite specific mass of the dispersed material. However, the value of the mass of the particles found from the experimental porosity distributions is nearly 20% larger than the value corresponding to $H_0 = 0.01$ m.

Figure 2 shows a two-dimensional pattern of time-averaged porosity distributions for the variant of Fig. 1b ($u_f = 0.544$ m/sec). As is evident from the figure we can distinguish integrally two zones in the bed: a region with a relatively weakly varying porosity extending from the bed base and to a level with a height of about 0.016 m; a region of sharp increase in porosity with height, extending from that level to the upper boundary of the bed. The time-averaged porosity cannot be considered homogeneous in the first zone despite the absence of large gradients of it. As is evident from the figure, there are particle accumulations near the chamber walls and the flow core is less loaded with the dispersed phase material. The concentration profile across the chamber width in the second zone is fairly homogeneous. Such a porosity distribution in the vertical channel is characteristic of fluidized beds [6] and is governed by the following reasons. Local regions of particle accumulation near the surfaces limiting the flow region form under the effect of their inhibiting action. The gas flow, tending to follow the line of least resistance, facilitates a decrease in porosity in the central part of the apparatus. This leads to a drop in velocity in the wall zones, which in turn ensures conditions favorable for downward motion of the particles near the apparatus walls. Therefore local zones of internal circulation of particles form in the middle portion of the bed near the limiting surfaces. These zones extend to a height above which the restrictive effect of the resistance of the suspended particle mass on the carrier medium flow is not as substantial as in the lower or the central portion of the bed.

Figure 3 shows the distributions, over height, of the porosity averaged over the bed cross section, corresponding to the case $u_f = 0.544$ m/sec, for three successive instants. As is evident from the figure, the bed height experiences distinct fluctuations of up to 30% of its time-averaged value. We point out that all the distributions presented in this figure refer to the stage where the state of the bed reaches a relatively stable regime of turbulent fluidization. Instantaneous patterns of particle distributions along the bed height show the presence of porosity fluctuations of large amplitude in the apparatus.

Figure 4 gives some idea of the character of the porosity pulsations and their amplitude. The time distributions of porosity values at two points located at different heights in the central portion of the bed, calculated for the layer fluidization rate $u_f = 0.76$ m/sec, are presented here. It is evident from the figure that one can immediately distinguish the determining frequency in the fluctuation structure, which is the same for both points. Its value is close to the frequency calculated on the basis of the relation [7]

$$\omega = \frac{1}{2\pi} \sqrt{g/L}, \quad (9)$$

where the smaller of the orthogonal dimensions of the bed $L = 0.01$ m is taken as the characteristic dimension. It also follows from the figure that fluctuations of larger amplitude are observed in the lower portion of the bed.

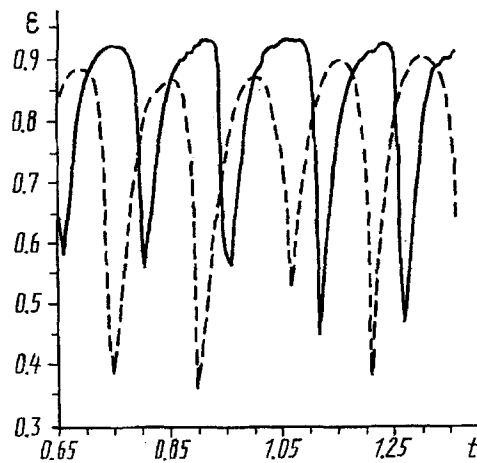


Fig. 4. Nonstationary behavior of the local porosity at the points with the coordinates (0.012 m; 0.0 m) - the solid curve and (0.005 m; 0.0 m) - the dashed one; $u_f = 0.76$ m/sec. t , sec.

In summary we point out that the mathematical model presented in this work makes it possible to reliably determine the basic characteristics of inhomogeneous fluidized beds (expansion rate, porosity distributions over height) and present the local and instantaneous values of all quantities characterizing the suspended state of the disperse system and analyze the structure of pulsations in FB on their basis.

NOTATION

t , time; x , y , Cartesian coordinates; α , ρ , p , volume fraction, density, pressure; U , V , velocity vector components; F_x , F_y , components of the interphase interaction forces; μ , viscosity factor; R , gas constant; g , free fall acceleration; Re , Reynolds number determined from the particle size and the phase slip; c_D , resistance coefficient; d_p , particle size; G , modulus of stresses in the particle medium; ρ^0 , true density of the medium; H , fluidized bed height; h , current coordinate reckoned along the height from the bed base; ω , frequency of porosity pulsations; δ_{ij} , Kronecker delta; u_f , fluidization rate; $\bar{\epsilon}$, porosity averaged over the channel width and time. Subscript: 1, carrier medium parameters; 2, dispersed phase.

REFERENCES

1. J. Yeats, Fundamentals of Fluidization Mechanics with Applications [Russian translation], Moscow (1986).
2. R. I. Nigmatulin, Fundamentals of the Mechanics of Heterogeneous Media [in Russian], Moscow (1978).
3. V. I. Ivanyutenko, N. V. Antonishin, and V. S. Nikitin, *Inzh.-Fiz. Zh.*, **11**, No. 3, 470-475 (1981).
4. Y. P. Tsuo and P. Gidasov, *AIChE J.*, **36**, 885-896 (1990).
5. S. Patankar, Numerical Methods for Solving Problems of Heat Transfer and Fluid Dynamics [Russian translation], Moscow (1984).
6. Fluidization [in Russian], Moscow (1991), p. 335.
7. O. M. Todes and O. B. Tsitovich, Fluidized Granular Bed Apparatuses [in Russian], Leningrad (1981).